Structural Evaluation of the Failure of the Harrison Road Bridge over the Great Miami River

D. R. SCHELLING, C. C. FU, AND V. RAGAVAN

On May 26, 1989, a pile bent and a two-span segment of the temporary bridge that carries Harrison Road over the Great Miami River collapsed. A passenger car fell into the river, causing the drowning of two occupants. Numerous sources confirm that the river, which was in high flood, carried a large amount of debris of various sizes and configurations. According to witnesses' statements, floating debris struck the pile bent, causing it to fail suddenly, bringing with it two sections of the superstructure. A study was commissioned by the National Transportation Safety Board (a) to provide a detailed analysis of the causes and sequence of failure of the structural elements contained within the temporary pile bent and superstructure; (b) to conduct an in-depth review of alternate analyses used to ascertain the causes of failure; (c) to provide recommendations as to the procedural issues which have surfaced due to the failure; and (d) to provide an evaluation of the pile bent with respect to conformance to the AASHTO *Standard Specifications for Highway Bridges*. The results of the study identify various factors that influenced the failure of the pile bent. These include the lack of quantitative guidelines under AASHTO for the determination of frequency and size of floating debris, variances allowed for the design and construction of temporary bridge structures, design procedures for determination of dynamically applied debris forces, and the rating of pile bents under hydrostatic, debris, and line-loading conditions.

In 1987, Hamilton County made a decision to replace an existing 440-ft-long simple-span through-truss with a new bridge over the Great Miami River at Miamitown, Ohio. On May 7, 1987, a consultant firm was commissioned to design the replacement bridge. It was decided to construct a temporary bridge until the new replacement bridge was complete and open.

The contractor submitted a proposal for the construction of both the permanent and temporary bridges on the basis of the consultant's designs and was selected as the successful bidder. Thereupon, the contractor submitted an alternate design for the temporary bridge after award, which is shown in detail in Figure 1. Comparison of the original consultant's design (Figure 2) with the alternate design recommended by the contractor as shown in Figure 1 indicates that the two designs are markedly different in the following respects:

1. The consultant's temporary structure is a three-dimensional frame with bracing positioned to resist lateral loads in two directions. The pier bent designed and constructed by the contractor is a plane frame with bracing positioned to withstand in-plane loads only.
2. The consultant's design exhibited larger members for both the columns and bracing than the contractor's design. Further, the consultant's design had 10 pile bent members as opposed to 4 members provided in the contractor's design. Finally, the consultant's design incorporated a greater amount of lateral bracing than the contractor's design.
3. The consultant's design provided for a much larger pile cap in both section and width than did the contractor's design.

Department of Civil Engineering, University of Maryland, College Park, Md. 20742.

The geometric and structural data that were used in the analysis of the temporary pile bent under the various loads were provided by the National Transportation Safety Board (NTSB) (*1–4*). The basic information relative to the pre- and postfailure conditions is shown in Figures 1 and 2 (*1*).

The actual grade of steel that was used in the construction of the pier bent was uncertain. Values of 36 ksi (i.e., A36 steel) were used for the yield strength in the FHWA, the contractor, and the contractor's consultant analyses. However, metallurgical tests indicate that the grade of steel that was actually used to construct the pile bent was Grade 50. However, because of a potential conflict regarding the value of the yield strength, values of 36 and 50 ksi were both used in the analysis.

Nine locations where the pile sections failed because of the formation of plastic hinges were evident. Table 1 presents the points where failure was indicated in the welds that connected the bracing to the pile members.

STATIC ANALYSIS PROCEDURES

Contained within this section is a definition of the static analysis procedures used to define the critical load conditions and modes of failure of the temporary pile bent. The independent investigation was conducted to assess the causes of failure. The presented analysis, termed the comprehensive analysis, investigated two separate failure modes using a nonlinear three-dimensional finite element analysis.

The objective of the comprehensive analysis is to provide the most appropriate analytical procedures to define most accurately the loading conditions and the manner in which the pile bent failed. In order to meet this objective, the following criteria were used:

1. The most realistic geometric parameters, structural modeling procedures, loading conditions, and material properties were used to replicate the conditions at the time of failure.

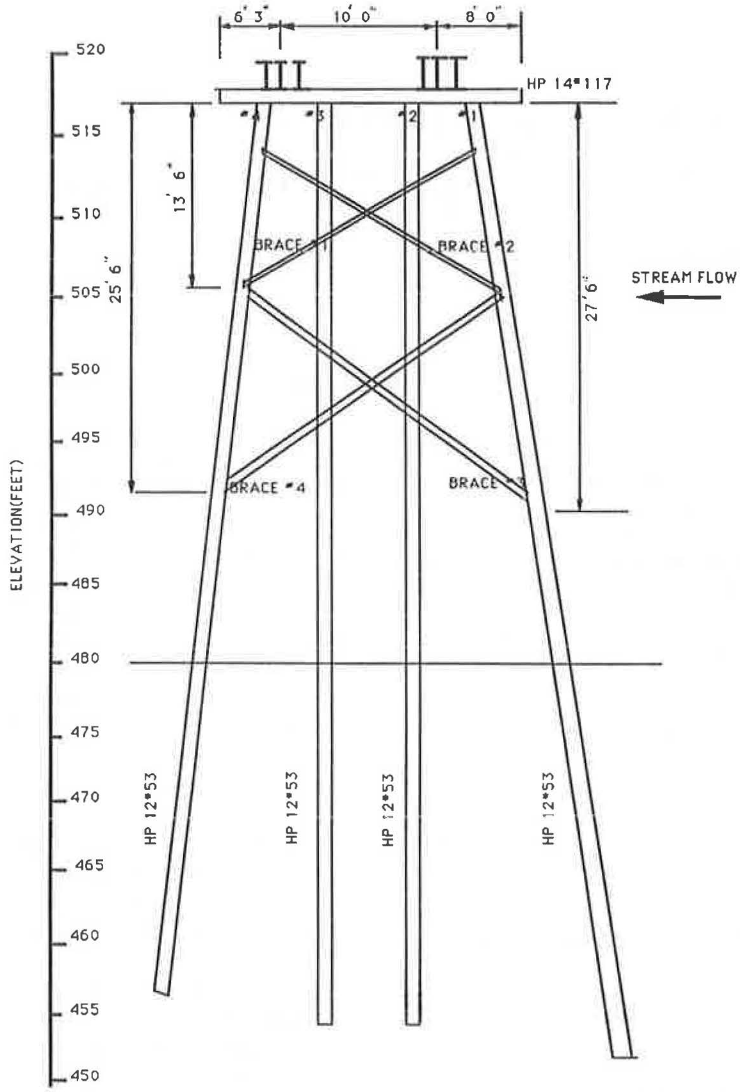

FIGURE 1 Elevation of pile bent (as constructed).

2. The pile bent was analyzed as a system incorporating all influential structural components.

3. The pile bent was investigated with respect to all appropriate and realistic failure modes. These modes were compared to the conditions influencing the bent before and during failure as well as with the postfailure bent configuration as determined by field measurements.

4. Where the prefailure bent parameters, modeling procedures, and postfailure data indicate uncertainty, a range of values was assumed.

Pile Bent Configurations

A series of eight pile bent configurations was subjected to analysis to determine the most probable sequence of failure of the various members and connections contained within the pile bent. Here, a series of three basic configuration types was identified and is defined as follows:

Config ID	*Description*
COR(*I,J*)	The undamaged pier configuration as originally constructed
CPF(*I,J*)	The pile bent at the prefailure condition. Here, various bracing hinges have formed but the damaged pile bent is still capable of sustaining additional load
CCA(*I,J*)	The pile bent is near or at the state of collapse. Here, numerous hinges have formed, large deformations are evident, and bracing connections have failed

For these configurations, the following indices are defined:

Index	*Value*	*Description*
I	1	Modeling with the superstructure included
	2	Modeling with the superstructure not included
J	1	Pier bent with material yield (Fy) of 50 ksi
	2	Pier bent with material yield (Fy) of 36 ksi

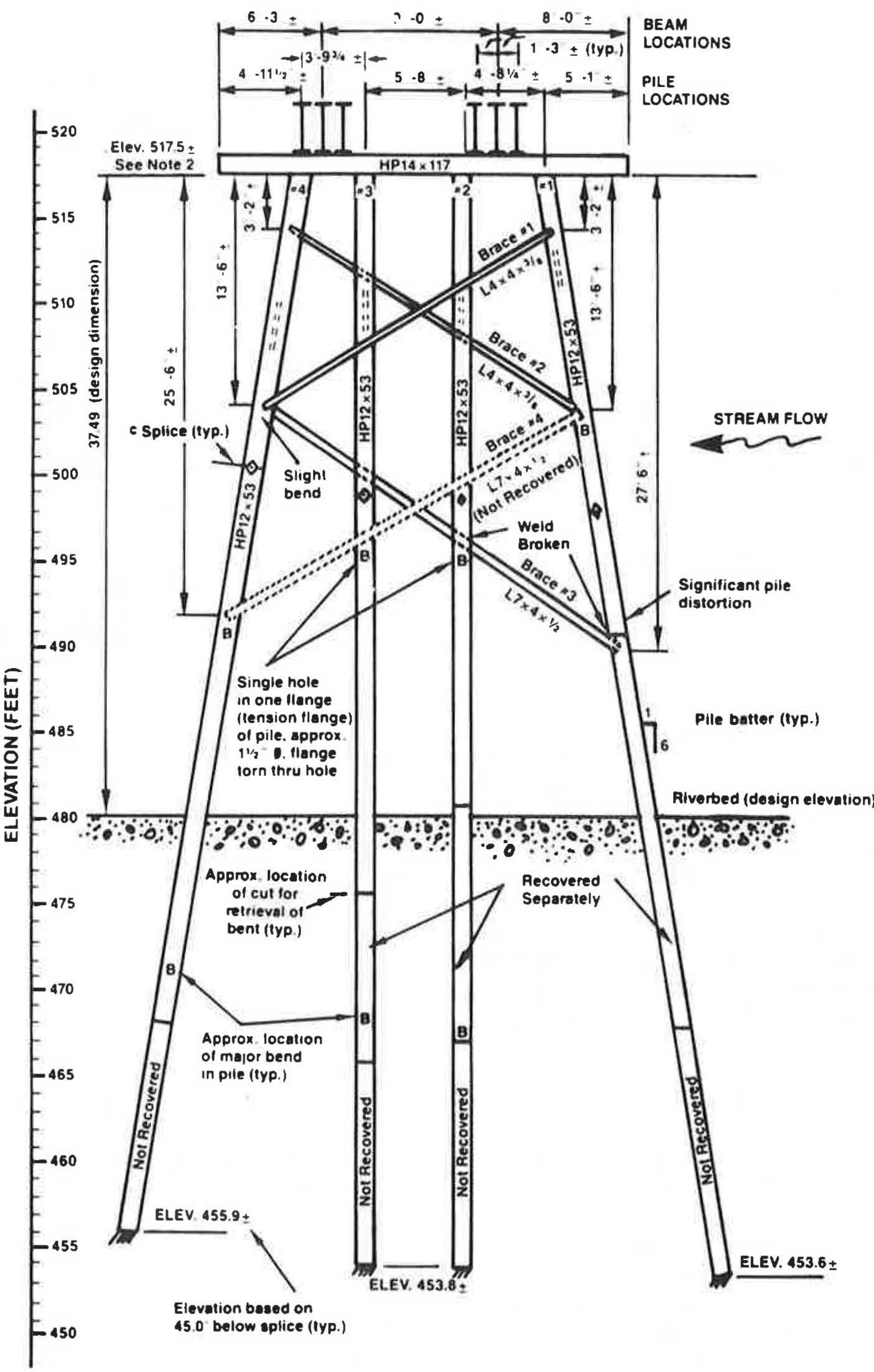

Notes: 1) This drawing based on measurements of salvaged materials.
2) Pier cap elevation based on construction plans.
3) B = Location of bend

FIGURE 2 Elevation of pile bent (postfailure) looking west (east face up).

TABLE 1 POINTS OF FAILURE OF PILE BENT SECTIONS

Pile Number	Brace Number	Hinge Id[a]	Approximate Elevation	Node ID	Comments
1	2	H_{12}	503′	33	Point of application of debris loading
1	3	H_{13}	491′	45	Weld broken
2	3	H_{23}	495′	42	Weld broken; flange containing hole was ruptured
2	–	H_{2G}	468′	50	Approximate fixity point for Pile 2
3	4	H_{34}	495′	43	Flange containing hole was ruptured
3	–	H_{3G}	468′	51	Approximate fixity point for Pile 3
4	1	H_{41}	504′	36	Small bend *(1)*
4	4	H_{44}	491′	48	
4	–	H_{4G}	472′	52	Approximate fixity point of Pile 4

[a]The notation H_{ij} refers to the location of a hinge occurring within the *i*th pile at the *j*th bracing point. When the *j*th bracing point is denoted by G, then the location is at the fixity point of the pile below the midline.

Analysis Components

Two types of analysis were conducted that involve the determination of the lateral load capacity and the sequence of failure from both buckling and elastoplastic-type failures.

First, a stability analysis was performed to determine the capacity and the various column failure modes of the overall structural pier bent system. The results of this analysis were compared with the previously conducted FHWA and the contractor's analyses because they also assumed column-type failure modes. This stability analysis type is often referred to as an eigenvalue buckling or bifurcation analysis. The procedure is conducted by mathematically determining the eigenvalues of the stiffness matrix that represent the critical deformed shapes of the various interconnected structural elements contained within the pile bent system. The load that represents the lower bound of the load capacity from all the various critical member configurations as determined from the eigenvalue analysis is the critical load for the structure.

The second analysis consisted of a determination of capacity and the failure modes of the pile bent caused by the formation of hinges. These occur sequentially throughout the structure as the lateral debris loading is incremented and lead to the overall failure of the bent. The formation of these hinges is characterized as follows *(5–7)*

1. They occur at locations of high moment that exceed the capacity of the section;
2. The hinge itself is caused either by the complete plastification of the section (a plastic hinge) or by buckling of the column element, or by their combination;
3. The formation of a hinge and the moment that initiates its formation may be markedly influenced by the combination of high deformations and axial compressive loadings that occur simultaneously within a member (e.g., P-Delta effects);
4. The formation of any hinge results in the redistribution of moment and forces throughout the entire pile bent. This is caused by the weakening of the structure at the hinge location;
5. A formation of a hinge, in itself, does not indicate overall failure of the bent;
6. When the number of hinges that form within the pile bent exceeds those required for elastic stability, collapse occurs;
7. The formation of hinges generally results in high deformations at various locations throughout the pile bent.
8. The failure of the connections at the juncture of the superstructure and the pile bent could have occurred any time after the formation of the first set of hinges early in the failure sequence. The separation of the superstructure from the pile cap opens the potential for the collapse of the superstructure before the overall failure of the pile bent itself.
9. An elastoplastic analysis is required for the determination of the behavior of the pile bent under the formation of hinges.

A summary of the definition of the column buckling and the elastoplastic mechanism methods used in the comprehensive analysis of the failure of the pier bent are presented in Table 2.

Loadings

The loading components that were applied to the pier bent for analysis of the modes of failure were determined through information supplied by NTSB *(1–4)* and checked by the authors. The components fall into four categories, which are described as follows.

Dead Loading

The dead loads are composed of the pile bent self-weight and that applied to the bent from the superstructure. The value of the dead-load intensities were determined through an evaluation of the various members and components as indicated in the plans compiled by NTSB *(1)*.

Live Loading

The live loads were assumed to consist of two cars weighing 12,000 lb positioned directly over Bent 2.

Stream Flow

The loading on the pile bent caused by stream flow is applied as a varying load increasing linearly with depth. A stream velocity of 9 ft/sec was assumed with a full stream force acting on the upstream leg of the bent, 75 percent of the full stream force on the inner legs and no stream force on the downstream leg. The reduction of the force from stream flow on the down-

TABLE 2 DEFINITION OF ANALYSIS COMPONENTS

PIER CONDITION					PURPOSE/METHODOLOGY/ASSUMPTIONS
TITLE (SOURCE)	ANALYSIS ID	F_y (KSI)	PIER CONDITION	L_s	
COMPREHENSIVE ANALYSIS (Authors)	COLUMN BUCKLING FAILURE (CB)	(a)	Original (COR) Prefailure (CPF)	10′	PURPOSE: To determine the global buckling capacities of all the members within the pile bent under various conditions. METHOD: A determination of the eigenvalues of the overall pile bent utilizing 3-D Frame analysis. ASSUMPTIONS: All those inherent within an eigenvalue analysis: 1) Linear elastic material 2) Small deformations 3) Failure occurs by Euler buckling
	ELASTO-PLASTIC FAILURE (EP)	36,50	Original (COR) Prefailure (CPF) Collapse (CCA)	10′	PURPOSE: To determine the capacity and sequence of failure of the pile bent under the incremental application of lateral loads. METHOD: A determination of the loads which will cause full plastification and/or local buckling at various locations throughout the bent utilizing 3-D frame via ANSYS. ASSUMPTIONS: 1) Elasto-plastic material 2) Moment magnification due to large deflection of structure (e.g., P-effects). 3) Moment/rotation values limited by controlling Mp and local buckling. 4) Yield condition is based on the predetermined stress-strain curves based on the unbraced length. 5) The dead, live and stream loads are all staying constant while debris loads increase incrementally. 6) Debris loads must be applied incrementally in order to determine connection failures.

stream pile bent legs is caused by estimated hydrologic shielding effects (*8–10*).

Debris Loading

The debris loading as applied to the pile bent is assumed to be a concentrated force applied upstream at elevation 502 ft. Although a range of values can be assumed including a potentially more severe elevation of 503.5 ft, all values are approximate (FHWA and the contractor assumed an elevation of 499.5 ft) with no elevation being found to be the most accurate. Further, no value of the intensity or exact characterization of the debris loading that caused the failure can be accurately established from field observations. For these reasons, the debris loading is incrementally applied to the pile bent models until failure is indicated and three characterizations of the debris loading are investigated, as follows:

1. The debris loading as applied gradually until failure occurs;
2. The debris loading as applied as a single floating mass that impacts the pile bent and causes sudden failure; and
3. A combination of these loadings.

Loading Spectrum

The loading cases that were used in the comprehensive analysis for determining the causes of failure are presented in Table 3. As indicated in Table 3, a total of 24 case combinations was considered, each requiring over 12 increments of load. Thus, well over 300 individual cases were considered in determining the sequence of failure and the central load combination that caused the failure.

Structural Model

The finite element method was used to determine the response of the pier bent to the loads applied. The definition of the nodes and connectivities (members) that define the modeling of the pier bent is shown in Figure 3. The specific capabilities of the finite element procedures are described as follows:

1. The pier bent is modeled as a three-dimensional frame using prismatic beam elements to represent the members;
2. Geometric nonlinearities caused by large deformations are considered;
3. Material nonlinearity is considered in the form of an elastoplastic idealization; and
4. The elastic buckling analysis uses eigenvalues to determine the critical lateral load intensities.

Pile Fixity

Wet medium sand is assumed to calculate the pile bent fixity locations (*4*). For a wider range of sand material, the fixity location may vary from 7 to 12 ft, and an average embedment distance of 10 ft is assumed.

DYNAMIC ANALYSIS PROCEDURES

The dynamic analysis consists of modeling the pier bent as an equivalent spring system with respect to the application of a lateral load at the water surface (i.e., the Node 33, see Figure 3). Here, the solution of a structurally equivalent one-degree-of-freedom spring mass system is used to represent the impact of a floating mass with the pier bent. Although

TABLE 3 DEFINITION OF ANALYSIS CASES

TITLE (Source)	CASE COMBO	ANALYSIS		LOADING CONDITIONS				PIER MODELS			
		ANALY ID	DESC	LDG ID	DL + LL	SF	DEBRIS	CONFIG ID	F_y KSI	Super Str.	Failure Status
COMPREHENSIVE ANALYSIS	1.1[1]	CB	Buckl ng	LC1	DL	None	Inc to Failure	COR 1.1	50	With	Pre Failure
	1.2[1]	CB	Buckl ng	LC1	DL	None	Inc to Failure	COR 2.1	50	W/O	Pre Failure
	1.3[1]	CB	Buckl ng	LC1	DL	None	Inc to Failure	CPF 2.1	50	W/O	Intermediate
	1.4	CB	Buckl ng	LC1	DL	None	Inc to Failure	COR 1.2	36	With	Pre Failure
	1.5	CB	Buckl ng	LC1	DL	None	Inc to Failure	COR 2.2	36	W/O	Pre Failure
	1.6	CB	Buckl ng	LC1	DL	None	Inc to Failure	CPF 2.2	36	W/O	Intermediate
	1.7[1]	CB	Buckl ng	LC2	DL+2Cars	Yes	Inc to Failure	COR 1.1	50	With	Pre Failure
	1.8[1]	CB	Buckl ng	LC2	DL+2Cars	Yes	Inc to Failure	COR 2.1	50	W/O	Pre Failure
	1.9[1]	CB	Buckl ng	LC2	DL+2Cars	Yes	Inc to Failure	CPF 2.1	50	W/O	Intermediate
	1.10	CB	Buckl ng	LC2	DL+2Cars	Yes	Inc to Failure	COR 2.2	36	With	Pre Failure
	1.11	CB	Buckl ng	LC2	DL+2Cars	Yes	Inc to Failure	COR 2.2	36	W/O	Pre Failure
	1.12	CB	Buckl ng	LC2	DL+2Cars	Yes	Inc to Failure	CPF 2.2	36	W/O	Intermediate
	2.1[1]	EP	Hinges	LC2	DL+2Cars	None	Inc to Failure	COR 1.1	50	With	Pre Failure
	2.2	EP	Hinges	LC2	DL+2Cars	None	Inc to Failure	COR 2.1	50	W/O	Pre Failure
	2.3	EP	Hinges	LC2	DL+2Cars	None	Inc to Failure	CPF 2.1	50	W/O	Intermediate
	2.4[2]	EP	Hinges	LC2	DL+2Cars	None	Inc to Failure	CCA 2.1	50	W/O	Collapse
	2.5	EP	Hinges	LC2	DL+2Cars	None	Inc to Failure	COR 1.2	36	With	Pre Failure
	2.6	EP	Hinges	LC2	DL+2Cars	None	Inc to Failure	COR 2.2	36	W/O	Pre Failure
	2.7	EP	Hinges	LC2	DL+2Cars	None	Inc to Failure	CPF 2.2	36	W/O	Intermediate
	2.8[2]	EP	Hinges	LC2	DL+2Cars	None	Inc to Failure	CCA 2.2	36	W/O	Collapse
	3.1	CB	Buckl ng	LC3	AASHTO	Yes	AASHTO	COR 2.1	50	W/O	Chk Design
	3.2	CB	Buckl ng	LC3	AASHTO	Yes	AASHTO	COR 2.2	36	W/O	Chk Design
	3.3	EP	Hinges	LC3	AASHTO	Yes	AASHTO	COR 2.1	50	W/O	Chk Design
	3.4	EP	Hinges	LC3	AASHTO	Yes	AASHTO	COR 2.2	36	W/O	Chk Design

[1] Evaluated but nongoverning.
[2] Governed by CPF analysis; model replaced.

the characterization of such an analysis is approximate, it does yield qualitative results that provide insight into the basic behavior of the pier under impact loading. Both force method and energy method were used to investigate the pile bent under impact. The limiting assumptions of such an analysis are summarized as follows:

1. The mass of the pier, in the force method, is neglected; this assumption tends to overestimate the effect of impact.
2. In the force method, the nonlinear shape of the spring displacement function is assumed to be linear; this assumption overestimates the strength of the pier bent.
3. The hydrodynamic mass, which tends to increase the effect of the impact, is neglected; this assumption tends to underestimate the effect of the impact.
4. Damping effects are neglected; these are felt to be inconsequential.
5. The hydrodynamic force on the mass after impact is neglected. This force could have had a significant effect on increasing the rate of failure of the pier bent.
6. The impact of the mass is assumed to be applied to Node 33 acting in the plane of the pier bent frame throughout the entire time history of failure.

Force Method

A spring-mass system can be represented by the following equation (*11*):

$$\ddot{y} + \lambda^2 y = F(t) \tag{1}$$

where y is the lateral displacement of the floating mass at the debris line (e.g., at Joint 33), $F(t)$ is the force of the water on the debris, and $\lambda^2 = K/M$, where K is the spring constant at the debris line as shown graphically in Figure 4 for the entire range of forces to failure and M is the mass of the floating object.

The assumptions regarding the variables and the boundary conditions for the solution of Equation 1 are as follows:

1. The initial displacement of the mass of the floating debris is given by $y(0) = 0$;
2. The initial velocity of the floating debris is given by $\dot{y}(0) = V_s$, the velocity of the streamflow (9 ft/sec);
3. The mass of the pier bent is neglected;
4. The force of the streamflow is neglected;
5. The density of the floating debris is taken as that of wood, $\rho_w = 0.05$ kg/ft^3;
6. The spring constant, K, will be taken as the initial value of the stiffness of the pier bent, $K = 11.4$ kips/in.;
7. The time of the impact is given by $t = \pi/2\lambda$; and
8. The length of the floating logs as observed is taken as 50 ft (*1*).

From these assumptions, the governing equations of motion are as follows:

$$y = (V_s/\lambda)\ \sin(\lambda t) \tag{2}$$

$$F = M\ddot{y} \tag{3}$$

where F represents the force of the floating mass on the bent and y is the acceleration of the floating mass. The maximum deformations and accelerations occur for $\lambda t = \pi/2$. Therefore, the maximum force F_m is represented by

$$F_m = M\lambda V_s \tag{4}$$

$$M = F_m^2/(V_s^2 K) = W_1/g \tag{5}$$

where W_l is the weight of the floating debris, which is idealized as a log.

$$W_l = F_m^2 g/(V_s^2 K) \tag{6}$$

$$D_l^2 = 4W_l/(\pi L \rho) \tag{7}$$

where D and L represent the diameter and the length, respectively, of the floating log of density ρ.

Energy Method

If the interface forcing function is known, the target structure can be modified mathematically to predict the structural response. Because of lack of information to define a forcing function, energy balance technique is used to estimate structural response.

The impact may be either elastic or plastic. The latter is characterized by the object's remaining in contact with the target subsequent to impact. In elastic impact, it disengages because of the elastic interface restoring force. On the basis of the available information and observation, the debris remains intact with the structure after impact, so the plastic formula is used.

The assumptions for velocity after impact are (a) the duration of the impact is short, and (b) the corresponding spring force is small. Then the velocities of the object and target are given by following equations,

$$V_m = V_s (M_m - eM_e)/(M_m - M_e) \tag{8}$$

$$V_t = V_s M_m (1 + e)/(M_m + M_e) \tag{9}$$

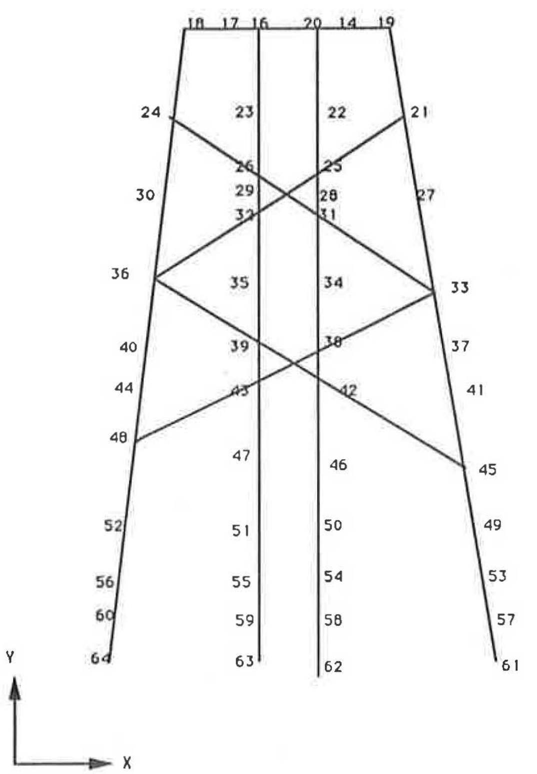

FIGURE 3 Definition of nodes.

The assumption for the required target strain energy capacity for plastic impact are (a) the coefficient of restitution e reduces to zero, and (b) the object and target attain the same velocity. Then the strain energy required is given by

$$E_s = (M_m V_m^2 + M_e V_t^2)/2 \tag{10}$$

From Equations 8 and 9,

$$V_m = V_t = M_m V_s/(M_m + M_e) \tag{11}$$

From Equations 10 and 11,

$$E_s = M_m^2 V_s^2 / 2(M_m + M_e) \tag{12}$$

Target Effective Mass

For distributed mass element, the effective mass, M_e, during impact varies with the deformed shape of the element during impact. The deflected shape during impact can be approximated by the shape of the first mode, which results in the following expression for M_e:

$$M_e = K/W^2$$

or

$$M_e = K(T_n/2\pi)^2 \tag{13}$$

where the value of K is obtained from the gradient of Figure 1. Finite element modal analysis for bridge substructure was performed to determine the natural frequency of the structure and the effective mass of the target. Then the value of M_e was verified using Equation 13.

Elastic Target Response

$$R_x = KX$$

$$X_m = X_0 + (2E_s/K)^2 \qquad \text{when } X_m < X_e \tag{14a}$$

Elastoplastic Response

$$R_x = KX \qquad \text{when } 0 < X < X_e$$

$$R_x = KX_e = R_m \qquad \text{when } X_e < X < X_m$$

Then

$$X_m = E_s/K(X_e - X_0) + (X_e + X_0)/2 \tag{14b}$$

SUMMARY OF RESULTS

The results of the sequence of failure that most conform to the basic criteria defined before is that given by the elastoplastic failure analysis (see Table 3) that was performed as part of the comprehensive analysis. Here, the lateral debris loading is applied incrementally, and the effect of each increment is checked for the failure of any component (e.g., piles, connections, and bracing). From this procedure, the following analysis results are obtained as a function of the lateral load intensity:

1. The moments, shears, axle forces, torsion (i.e., the stress resultants), and deformation at each joint;
2. The location of plastic hinges;
3. The failure of any structural component within the pile bent;
4. The level of redistribution of the stress resultants caused by the formation of hinges, along with the failure of any weldment that connects the cross bracing to the pile bent system;
5. The equivalent lateral spring constant of the pile bent at the point of application of the debris loading;
6. The lateral deformations at the beam seat locations; and
7. The value of the intensity of the debris loading when theoretical collapse occurs.

The sequence of the response of Pile Bent 2 to an incrementally applied debris loading is presented in Table 4 for yield strengths of 36 and 50 ksi. The sequence of response represented by the events presented in Table 4 may define the complete load response history of the pile bent. Detailed in Table 4 is a summary of the load levels at which the bracing failed, the sequence and location of the formation of plastic hinges, the deformation at the point of application of the debris and at the top of the pile bent, and, finally, the equivalent stiffness (e.g., the spring constant) of the pier bent system. This spring constant is shown in Figure 4 for the full range of loadings and deformation to failure. From the results of the analysis, the following conclusions can be drawn:

1. The postfailure configuration of the pile bent as documented by NTSB (*1*) conforms to the locations of the hinges predicted by the elastoplastic failure analysis. A summary of the correlation of the hinges from analysis and from field observations is presented in Table 5.
2. The failure of Pile Bent 2 was initiated at a debris loading of about 15 kips for both yield strengths of 36 and 50 ksi by using the elastoplastic method.
3. The intensity of the lateral debris loading required for overall collapse ranged from about 20 to 22.5 kips for a yield strength of 36 ksi and more probable range of values of from 22.5 to 25 kips for a yield strength of 50 ksi.
4. The value of the lateral debris loading at which the connections that attach the superstructure to the pier bent failed and that caused the superstructure to fall off the pier seat is not known from analysis. (Because of the lack of data regarding the size and postfailure disposition of the beam seat connections, a quantitative analysis of the sequence of failure of the superstructure is not possible.) The intensity of the debris loading that caused the failure (falling) of the superstructure ranges from 15,000 to about 25,000 lb.
5. The influence of the superstructure on the overall lateral in-plane stiffness of the pile bent is negligible.
6. The superstructure elements provided a degree of stiffness adequate to prevent out-of-plane torsional movement of the pile bent as well as out-of-plane buckling of Pile (Column) 4.
7. In order to perform the elastoplastic analysis of the pile bent as a system, it is necessary to consider the interacting influence of all members including bracing elements. The alternate buckling analysis assumes that these are secondary non-load-carrying members with lower strength requirements. Examples of such differences as cited by AASHTO (*9,10*) for compression members are given as follows:

		Primary Members		*Secondary Members*	
Item	*AASHTO Ref.*	*Limit*	*Actual*	*Limit*	*Actual*
b/t	10.35.2.3 (Compression)	12	14	16	14
KL/r	10.7.1 (Compression)	120	94	140	137
L/r	10.7.5 (Tension)	200	94	240	137

The 14 actual primary tension members violate the AASHTO primary member requirements.

TABLE 4 PIER BENT STATUS FOR VARIOUS INTENSITIES OF DEBRIS LOADING

Fy (KSI)	DEBRIS LOADING (k)	PIER CONDITION																					LATERAL DEFORMATION			K_{33} (K/ft)
		Hinge Formation Joint List																			Status of of Bracing	Config ID	Joint 33 (IN)	Jt. 19 (IN)	Max/Joint (IN/Joint No)	
(1)	(2)	48	64	62	61	43	63	42	58	45	60	59	46	50	54	55	38	56	39	57	(4)	(5)	(6)	(7)	(8)	(9)
50	5.0																				Intact	COR2.1	.620	-0.58		136.8
	7.5																					COR2.1	.850	-0.65		136.8
	10.0																					COR2.1	1.053	-0.80		136.8
	12.5																					COR2.1	1.254	-0.96		136.8
	15.0		X	X	X																	COR2.1	1.497	-1.14	1.82/41	136.8
	17.5	X	X	X	X		X	X														CPF2.1	1.835	-1.40	2.22/41	Variable
	20.0	X	X	X	X	X	X	X	X	X	X											CPF2.1	2.500	-1.91	3.01/45	Variable
	22.5	X	X	X	X	X	X	X	X	X	X	X	X		X							CPF2.1	2.578	-2.72	4.33/45	20.7
	25.0	X	X	X	X	X	X	X	X	X	X	X	X		X							CPF2.1	4.872	-3.70	5.94/45	20.7
	27.5	X	X	X	X	X	X	X	X	X	X	X	X		X	X						CCA2.1	6.258	-4.74	7.66/45	20.7
	30.0	X	X	X	X	X	X	X	X	X	X	X	X		X	X					Failed	Unstable	7.763	-5.88	9.53/45	20.7
36	<15.0																				Intact	COR2.2				136.8
	15.0	X	X	X	X																	COR2.2			1.85/41	
	17.5	X	X	X	X	X	X	X	X	X												CPF2.2			2.31/41	Variable
	20.0	X	X	X	X	X	X	X	X	X	X											CPF2.2			3.29/45	Variable
	22.5	X	X	X	X	X	X	X	X	X	X	X	X	X	X							CPF2.2			4.73/45	20.7
	25.0	X	X	X	X	X	X	X	X	X	X	X	X	X	X							CCA2.2			6.38/45	20.7
	27.5	X	X	X	X	X	X	X	X	X	X	X	X	X	X	X	X					CCA2.2			8.20/45	20.7
	30.0	X	X	X	X	X	X	X	X	X	X	X	X	X	X	X	X	X	X	X	Failed	Unstable			10.73/45	20.7

Notes: a) Values have been used from Fy = 50 case since the overall stiffness for Fy = 36 is almost identical.

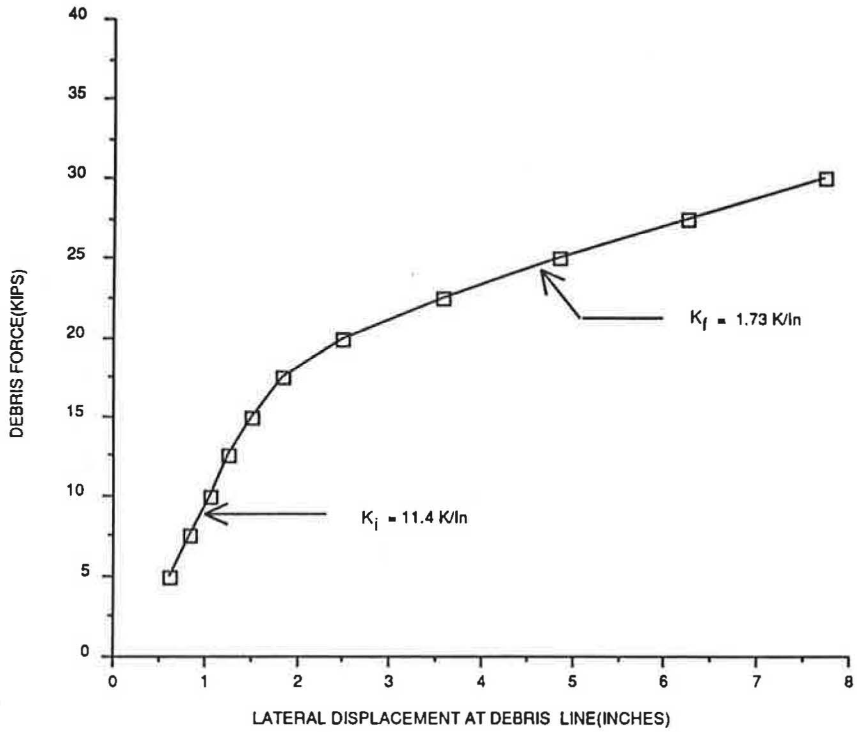

FIGURE 4 Debris force versus displacement for pile bent.

TABLE 5 COMPARISON OF RESULTS OF ANALYSIS AND FIELD OBSERVATION

ID	LOCATION				FIELD OBSERVATION	RESULTS OF ANALYSIS		
	Col. No.	Bracing No.	Node No.	Elevation		Fy (Ksi)	Formation of Hinge	Loading (k)
H_{12}	1	2	33	503′	Hinge with rotation of about 35°	50	None observed	(a)
H_{13}	1	3	45	491′	Severed		Hinge formation	17.5
H_{16}	1	-	61	468′	Member not recovered		Hinge formation	15.0
H_{23}	2	3	42	495′	Hinge location w/ tear & 90° rotation		Hinge formation	17.5
H_{2G}	2	-	62	468′	Severed		Combined plasticized	15.0
H_{2G}	2	-	58	468′	Severed		region for nodes 62 & 58	20.0
H_{34}	3	4	43	495′	Hinge location w/ tear & 90° rotation		Hinge formation	20.0
H_{3G}	3	-	63	468′	Severed		Combined plasticized	17.5
H_{3G}	3	-	59	468′	Severed		region for nodes 63 & 59	22.5
H_{41}	4	1	36	504′	Small bend observed (Ref 12)		None indicated	(b)
H_{44}	4	4	48	491′	Hinge location with 100° rotation		Hinge formation	17.5
H_{4G}	4	-	64	472′	Hinge location with 60° rotation		Combined plasticized	15.0
H_{4G}	4	-	60	472′	Hinge location with 60° rotation		region for nodes 64 & 60	20.0
H_{12}	1	2	33	503′	Hinge with rotation of about 35°	36	None observed	(a)
H_{13}	1	3	45	491′	Severed		Hinge formation	17.5
H_{1G}	1	-	61	468′	Member not recovered		Combined plasticized	15.0
H_{1G}	1	-	57	468′	Member not recovered		region for nodes 61 & 57	30.0
H_{23}	2	3	42	495′	Hinge location w/ tear & 90° rotation		Hinge formation	17.5
H_{2G}	2	-	62	468′	Severed		Combined plasticized	15.0
H_{2G}	2	-	58	468′	Severed		region for nodes 62 & 58	17.5
H_{34}	3	4	43	495′	Hinge location w/ tear & 90° rotation		Hinge formation	17.5
H_{3G}	3	-	63	468′	Severed		Combined plasticized	17.5
H_{3G}	3	-	59	468′	Severed		region for nodes 63 & 59	22.5
H_{41}	4	1	36	504′	Small bend observed (Ref 12)		None indicated	(b)
H_{44}	4	4	48	491′	Hinge location with 100° rotation		Hinge formation	15.0
H_{4G}	4	-	64	472′	Hinge location with 60° rotation		Combined plasticized	15.0
H_{4G}	4	-	60	472′	Hinge location with 60° rotation		region for nodes 64 & 60	20.0

8. When resisting lateral forces, the pier bent actually performs as a frame with the non-pile-bracing members acting as main load-carrying members and not as bracing per se. In such cases, it would be prudent to design the bracing members as primary members because the lateral loads most often govern the design.

9. The holes that exist at Nodes 42 and 43 on one side of the flanges of each column member have caused the increase of stress adjacent to the holes (i.e., stress concentrations or stress raisers). Such increases in stress have resulted in the tensile failure of the flange material from the hole to the outer edge of the flange.

The separation of the material at Nodes 42 and 43 may have caused a low-to-moderate weakening of the pile bent as compared with the results obtained from an analysis of the pile bent with no holes.

10. It has been determined that the pile bent does not meet the strength requirements for even a minimal lateral load intensity caused by waterborne debris.

11. The original design submitted by the consultant may have represented a much more appropriate design, with respect to the capacity to resist lateral loadings such as those caused by floating debris.

The results of a dynamic analysis of the pile bent subjected to a floating mass impacting at the water level are presented in Table 6. These results were generated from the solution of a spring mass system. Here, the weight of the maximum critical log, assumed to be 50 ft in length, along with the corresponding diameter of the log is given for yield strengths of 50 and 36 ksi. The results as summarized in Table 6 lead to the following conclusions:

1. An event characterized by a floating log 50 ft in length and ranging from about 7 to 14 in. in diameter impacting the pile bent at stream flow velocity is capable of providing the lateral impact force required for collapse of the pile bent.
2. If the pile bent were to be rated for an event characterized by the impact of a floating log, the rated log would be 50 ft in length and about 4 in. in diameter.
3. The most probable characterization of the debris that actually struck the pile bent and caused it to fail is a combination of impact and a constant force. A review of the types of debris shown on a video taken at the time of the flood indicates objects exhibiting both large surface areas and mass often interconnected together. A combination of hypothetical combinations of impact and constant force caused by hydrostatic effects is given as follows for a log 50 ft in length and 7 in. in diameter:

ID	*Surface Area*	*K*	V^2 *(ft/sec²)*	*Constant Force (kips)*	*Impact Force (kips)*	*Combined Force (kips)*
1	25	1.375	81	2.8	15.0	17.8
2	64	1.375	81	7.1	15.0	22.1
3	100	1.375	81	11.1	15.0	26.1
4	160	1.375	81	17.8	15.0	32.8

The *K* values originated in Article 3.18.1 (*9*).

Thus, even an object of minimal mass coupled with a surface area of 160 ft^2 (e.g., a dock about 8 ft deep and 20 ft long) can exert a combined force of over 32 kips, which is in excess of that required for collapse.

An evaluation of the pile bent structure was performed using the 1983 *Standard Specification for Highway Bridges* (*9*). This evaluation involved those provisions that would apply to steel pile bent support structures under the service load design method.

The results from the application of the AASHTO provisions for combined stresses for Column 4 given in Article 10.36 and Equations 10–41 and 10–42 for all applicable load group combinations are presented in Table 7.

A review of the summary indicates that three factors have influenced the performance of the pile bent:

1. Velocity of the stream flow in providing the inertia effects for floating debris;
2. The weakness of the pile to cross frame connections; and
3. The nonconformance of the pile bent design to the AASHTO specification.

Other factors that entered into the structural evaluation are either minor (i.e., depth to fixity, yield strength, and intensity of the dead and live loadings) or are unknown (i.e., the in-

TABLE 6 SUMMARY OF CRITICAL IMPACT CASES

LOAD IMPACT CASE		PIER BENT		LATERAL LOAD				MAX CRITICAL LOG		
ID	Description	Fy (ksi)	K (K/Ft)	Value (K)	F.S.	Time (sec)	Description	Weight (K)	Length (Ft)	Diam (Ft)
	FORCE METHOD:									
DL1.2.1	Rated value for debris loading	50	136.80	8.3	1.8	0.0106	Pre-failure cond.	.200	50	.32
DL1.2.2	Required for connection failure and formation first hinges	50		15.0	1.00	0.0191	Pre-failure cond.	.654	50	.58
DL1.2.3	Most probable upper limit	50		25.0	1.00	0.0319	Upper collapse value	1.816	50	.96
DL1.2.4	Most probable value at failure	50		22.5	1.00	0.0287	Lower collapse value	1.471	50	.87
DL1.2.5	Failure of weld at node 45						Collapse	2.615	50	1.15
DL2.2.1	Rated value for debris loading	36	136.80	8.3	1.8	0.0106	Pre-failure cond.	.200	50	.32
DL2.2.2	Required for connection failure and formation first hinges	36		15.0	1.00	0.0191	Pre-failure cond.	.654	50	.58
DL2.2.3	Most probable upper limit	36		22.5	1.00	0.0207	Upper collapse value	1.471	50	.87
DL2.2.4	Most probable value at failure	36		20.0	1.00	0.0255	Lower collapse value	1.162	50	.77
DL2.2.5	Failure of weld at node 45	36		30.0	1.00	0.0383	Collapse	2.615	50	1.15
	EQUIVALENT ENERGY METHOD:									
DL1.2.2	Required for connection failure and formation first hinges	50	136.80	15.0	1.00	---	Pre-failure cond.	2.46	---	---
DL2.2.2	Required for connection failure and formation first hinges	36	136.80	15.0	1.00	---	Pre-failure cond.	2.46	---	---

TABLE 7 SUMMARY OF RESULTS FOR THE AASHTO CODE CHECK (9) ON PILE BENT 2

AASHTO GROUP COMBINATIONS								RESULTS FOR PILE 4 (nodes 48-64)	
GROUP NO.	DL	L+I	SF	W	WL	ICE	% of Allowable Stress	Eq 10-41	Eq 10-42
I	1	1	1	0	0	0	100	Meet	Meet
II	1	0	1	1	0	0	125	Not meet	Not meet
III	1	1	1	.3	1	0	125	Not meet	Meet
IV	1	1	1	0	0	0	125	Meet	Meet
V	1	0	1	1	0	0	140	Meet	Meet
VI	1	1	1	.3	1	0	140	Meet	Meet
VII	1	0	1	0	0	0	133	Meet	Meet
VIII	1	1	1	0	0	1	140	Not meet	Not meet
IX	1	0	1	0	0	1	150	Not meet	Not meet

fluence of the holes in the flanges, the importance of the strength of the connections, and scour).

CONCLUSIONS

The primary causes of failure of the pile bent were the lack of structural capacity under the application of lateral loadings. Various indications were evident within the results developed herein that amply supported this conclusion, as follows.

- Field Survey. The postfailure configuration of the pile bent as determined by an NTSB field survey (*1*) indicated that the failure was caused by a lateral load. Further, a finite element analysis of the pile bent indicated that the level of lateral load required for a failure pattern that was virtually identical to that determined by field observation ranged from 22.5 to 25.0 kips. This correlation verifies that the computer model is predicting the basic behavior of the pile bent correctly.
- Pile Bent Configuration. The pile bent may have been proportioned to resist the vertically applied dead and live loads only. The factors to safety for such loadings were found to be high (3.8), as opposed to the factors of safety resulting from laterally applied loads, which were low, in some cases below 1.0 (i.e., they fell below the specified level of safety). Further, the placement of the lateral structural elements indicated that they were positioned to serve as bracing to strengthen the piles against in-plane buckling rather than to resist lateral forces.
- Code Check. The application of the combined group loadings to the pier bent indicated structural nonconformance to the AASHTO specifications. Specifically, the pile bent failed to meet the AASHTO requirements for Groups II, III, VIII, and IX, each of which contains high lateral load components that include load combinations resulting from stream flow, wind, wind on live loads, and ice. According to AASHTO, "The loading combinations shall be in accordance with Article 3.22" (*9*). Article 3.22 specifies, "Each component of the structure, or the foundation on which it rests, shall be proportional to withstand safely all group combinations of these forces that are applicable to the particular site or type" (Article 3.22) (*9*). Here, no qualifications are stated that limit these requirements for temporary structures.
- Computed Lateral Capacities. The capacity of the pile bent under the application of lateral loadings has been estimated under various criteria summarized as follows:

Criteria	*Lateral Load (kips)*
Nonlinear Analysis	
Rated lateral load capacity (FS = 2.12)	7.1
Lateral load to first yielding	15.0
Lateral load to collapse of superstructure	15.0–25.0
Lateral load to collapse	22.5–25.0
Impact of floating log (L = 50 ft, D = 7–14 in.)	22.5–25.0
Impact of floating log (L = 50 ft, D = 7 in.) plus hydrostatic force (area of 100 ft^2)	22.5–25.0
Standard Linear Frame Analysis for Pile Bent Failing Load Groups:	
II	25.4
III	17.3
VIII	25.0
IX	46.5

Load Group IX represents the maximum lateral load capacity provided by AASHTO. From this summary, the maximum values of the lateral load capacity that would have been provided by the pile bent if it had been proportioned to meet the AASHTO group loading requirements is as follows:

Group No.	*Factor of Safety*	*Failure Criterion*	*Analysis Method*	*Lateral Load Capacity (kips)*
IX	2.12	Eq. 10–41, 10–42 (*5*)	Linear	46.5
IX	1.00	Eq. 10–41, 10–42 (*5*)	Linear	~ 98.6
IX	1.00	Actual collapse	Nonlinear	~148 to ~165

Thus, the following is a comparison of the lateral load capacities of the pile bent as constructed and one that would have met the AASHTO group loadings:

	Lateral Capacity of Bent (kips)	
Failure Criterion	*Meeting AASHTO*	*As Constructed*
Nominal strength (FS = 2.12)	46.5	7.1
Nominal strength (FS = 1.00)	~98.6	15.0
Collapse strength	148-~165	22.5-25.0

Thus, a pile bent that meets the AASHTO group loading requirements is about 6.5 times stronger than that provided by the structure designed by the contractor. Further, the actual lateral load capacity that a pile bent that conforms to AASHTO is about 150 kips as compared to about 25 kips for the contractor's design. Such an increase in the lateral load capacity afforded by a design that would conform to the AASHTO group loadings would almost certainly have prevented failure.

GLOSSARY OF VARIABLES

b = width of flange;
D_1 = diameter of floating log;
e = coefficient of restitution;
E_s = strain energy of system;
$F(t)$ = forcing function during impact;
F_m = maximum force of floating mass;
g = gravity acceleration;
k = equivalent spring stiffness at Joint 33;
L = length of floating log, length of member;
M_e = effective mass of structural system;
M_m = mass of floating debris (object);
t = time of impact, thickness of flange;
T_n = calculated natural period of element;
V_s = velocity of stream flow;
V_m = velocity of floating debris (object);
V_t = target velocity;
W_1 = weight of floating debris;
X_e = yield displacement (at 15-kip debris load);
X_{or} = displacement caused by other load (without debris load);
X_m = maximum combined displacement;
Y = displacement (translation) in X direction;
r = radius of gyration; and
ω, λ = natural frequencies of systems.

REFERENCES

1. R. A. Weber. *Bridge Design and Construction.* Factual Report, National Transportation Safety Board, Washington, D.C., 1989.
2. M. A. McMurtry. *Hydrology and Geology.* Factual Report, National Transportation Safety Board, Washington, D.C., 1989.
3. Collins Engineers. *Underwater Inspection and Soundings of the Temporary Bridge over the Great Miami River at Miamitown, Hamilton County, Ohio.* Exhibit 3-B, Docket No. HY-510-89, National Transportation Safety Board, Washington, D.C., 1989.
4. H. C. Nutting Company. *Report of Geotechnical Investigation, Bridge Replacement on Harrison Pike over the Great Miami River, Miamitown, Ohio, Dated 1987.* National Transportation Safety Board, Washington, D.C., 1989.
5. *Specification for the Design, Fabrication and Erection of Structural Steel for Buildings*, Part II (Plastic Design), American Institute of Steel Construction, Inc., New York, Feb. 12, 1969.
6. A. P. Boresi and O. M. Sidebottom. *Advanced Mechanics of Materials*, 4th ed. John Wiley, New York, 1985.
7. Salmon and Johnson. *Steel Structures, Design and Behavior.* Harper and Row, New York, 1971.
8. *Manual for Maintenance of Bridges.* AASHTO, Washington, D.C., 1983.
9. *Standard Specifications for Highway Bridges*, 13th ed. AASHTO, Washington, D.C., 1983.
10. *Standard Specifications for Highway Bridges*, 14th ed. AASHTO, Washington, D.C., 1989.
11. C. H. Norris, R. J. Hansen, M. J. Holley, Jr., J. M. Biggs, S. Namyet, and J. K. Minami. *Structural Design for Dynamic Loads.* McGraw-Hill, New York, 1959.
12. *Analysis Sheets for the Evaluation of Pile Bent No. 2.* FHWA, U.S. Department of Transportation, 1989.

Publication of this paper sponsored by Committee on General Structures.